Supporting Information

Self-assembled Nanostructures of Optically Active Phthalocyanine Derivatives. Effect of Central Metal Ionic on the Morphology, Dimension, and Handedness

Ranran Sun,[a] Liang Wang,[b] Jing Tian,[a] Xiaomei Zhang*[a] and Jianzhuang Jiang*[b]

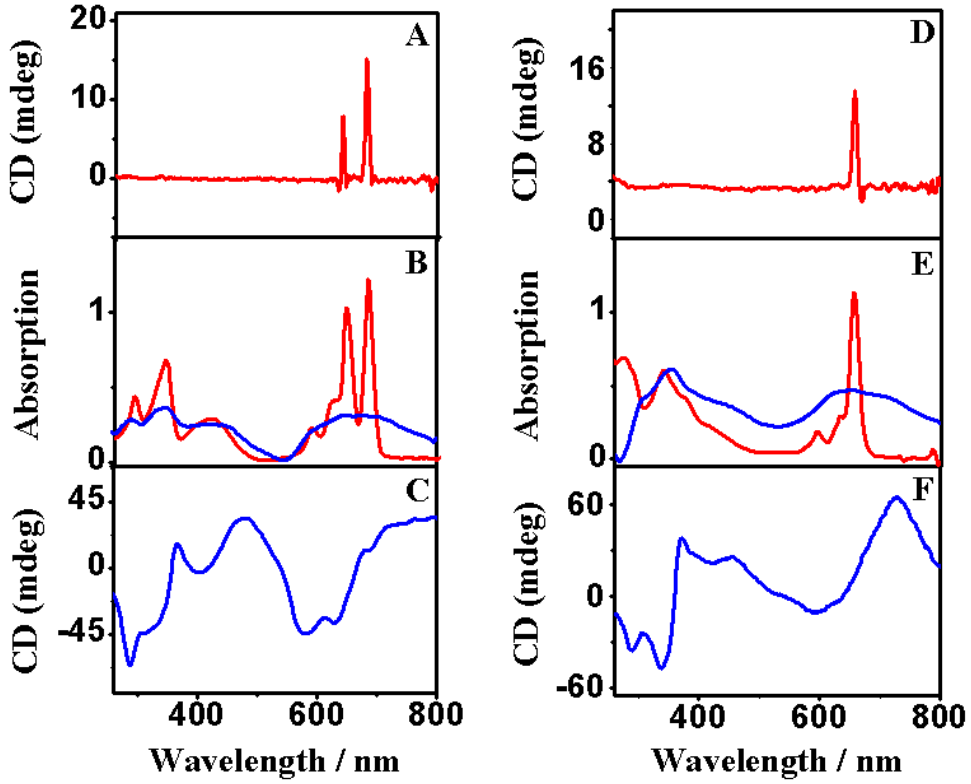

Figure S1. Electronic absorption and Circular Dichroism (CD) Spectra. CD spectra of (*S*)-$H_2Pc(\beta\text{-}OC_5H_{11})_8$ (**1**) in dilute chloroform solution (A); The electronic absorption spectrum of (*S*)-$H_2Pc(\beta\text{-}OC_5H_{11})_8$ (**1**) in dilute chloroform solution (red line) and **1** nanostructures dispersed in methanol (blue line) (B); CD spectra of **1** nanostructures dispersed in methanol (C); CD spectra of (*S*)-$ZnPc(\beta\text{-}OC_5H_{11})_8$ (**2**) in dilute chloroform solution (D); The electronic absorption spectrum of (*S*)-$ZnPc(\beta\text{-}OC_5H_{11})_8$ (**2**) in dilute chloroform solution (red line) and **2** nanostructures dispersed in methanol (blue line) (E); CD spectra of **2** nanostructures dispersed in methanol (F).

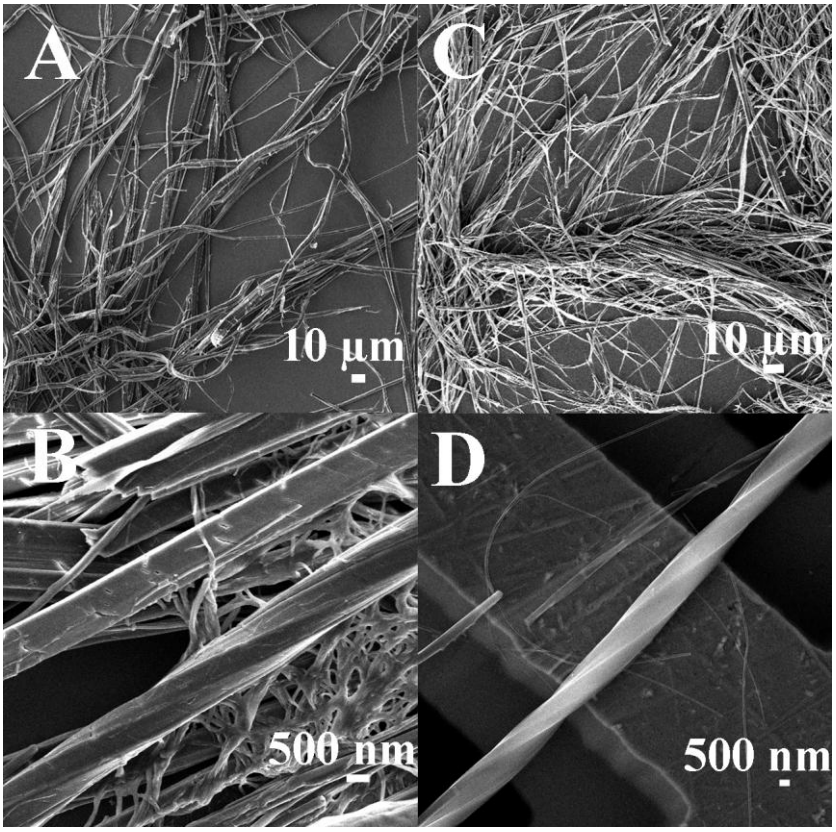

Figure S2. SEM images of self-assembled nanostructures fabricated from compounds **1**-**2**. Nanostructures fabricated from (*S*)-$H_2Pc(\beta\text{-}OC_5H_{11})_8$ (**1**) observed by SEM (A); High-magnification SEM image fabricated from **1** showing right-handed fibrous nanostructure (B); Nanostructures fabricated from (*S*)-$ZnPc(\beta\text{-}OC_5H_{11})_8$ (**2**) observed by SEM (C); High-magnification SEM image fabricated from **2** showing right-handed fibrous nanostructure. (D).

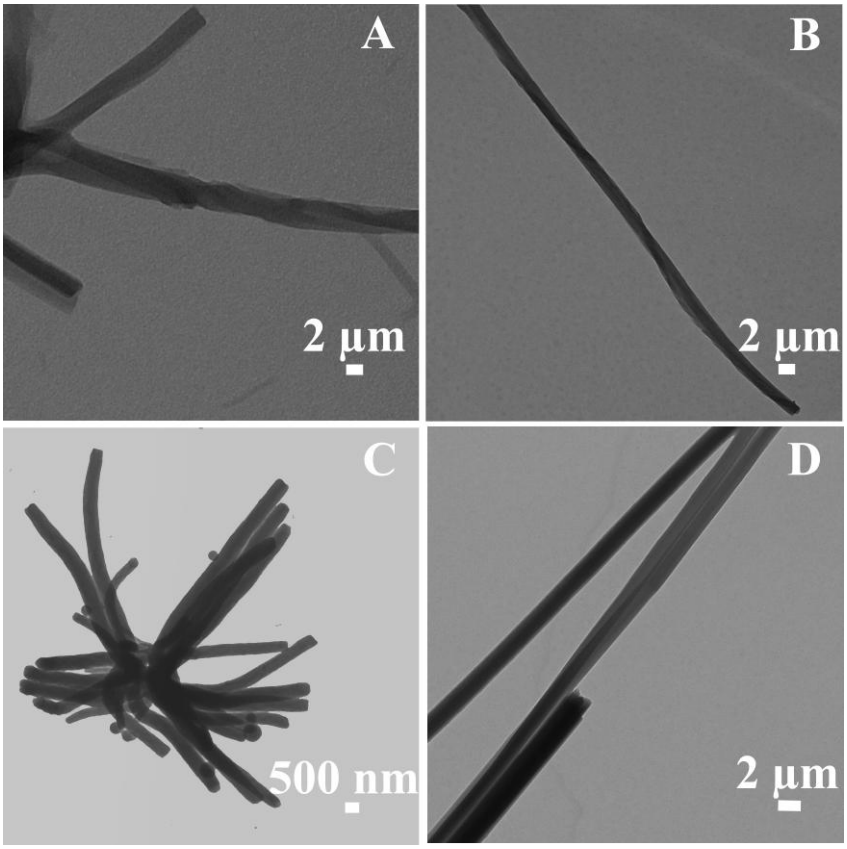

Figure S3. TEM images of self-assembled nanostructures fabricated from compounds **1**-**4**. Nanostructures fabricated from (*S*)-$H_2Pc(\beta\text{-}OC_5H_{11})_8$ (**1**) observed by TEM (A); Nanostructures fabricated from (*S*)-$ZnPc(\beta\text{-}OC_5H_{11})_8$ (**2**) observed by TEM (B); Nanostructures fabricated from (*S*)-$CuPc(\beta\text{-}OC_5H_{11})_8$ (**3**) observed by TEM (C); Nanostructures fabricated from (*S*)-$NiPc(\beta\text{-}OC_5H_{11})_8$ (**4**) observed by TEM (D).

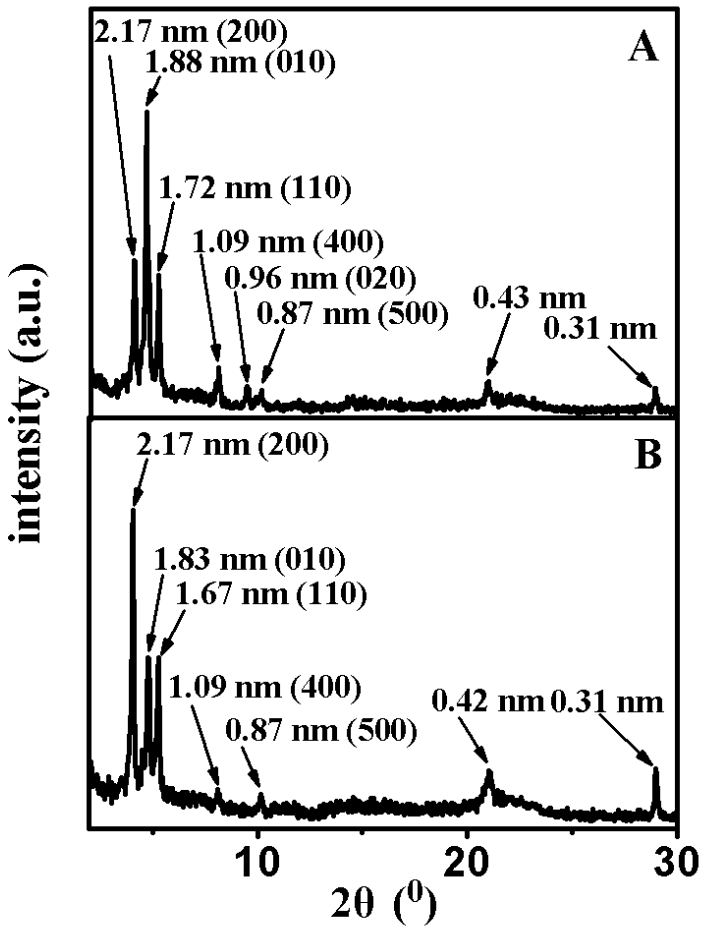

Figure S4. XRD profiles of the aggregates fabricated from **1** and **2** (A-B).

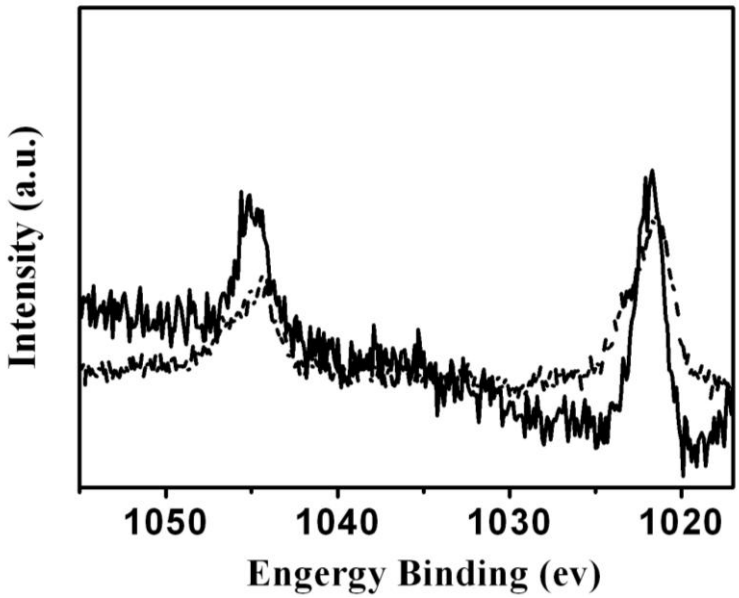

Figure S5. X-ray photoelectron spectra for complex **2** (solid line) and aggregates of complex **2** (dotted dash line) deposited on silicon surface.

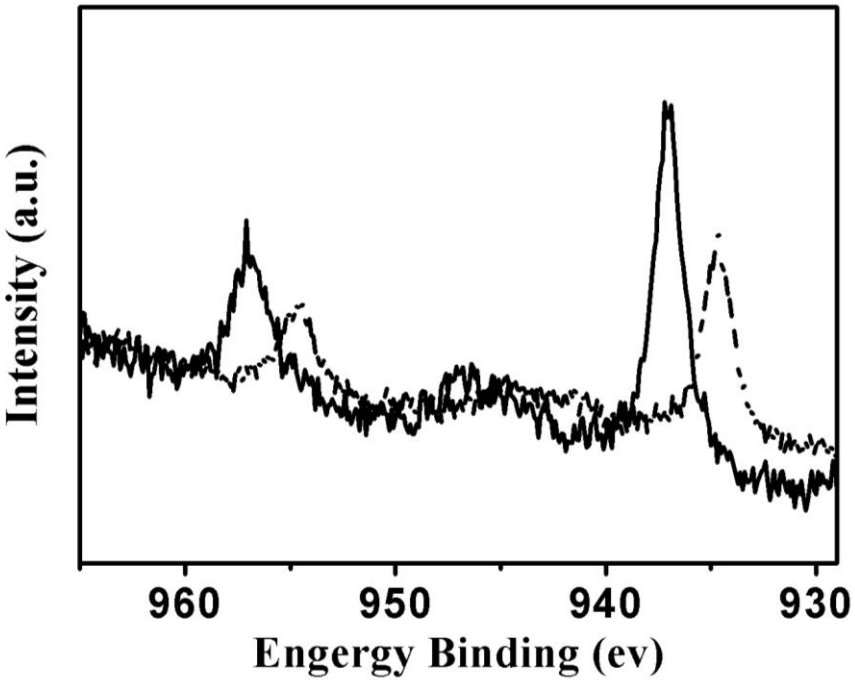

Figure S6. X-ray photoelectron spectra for complex **3** (solid line) and aggregates of complex **3** (dotted dash line) deposited on silicon surface.

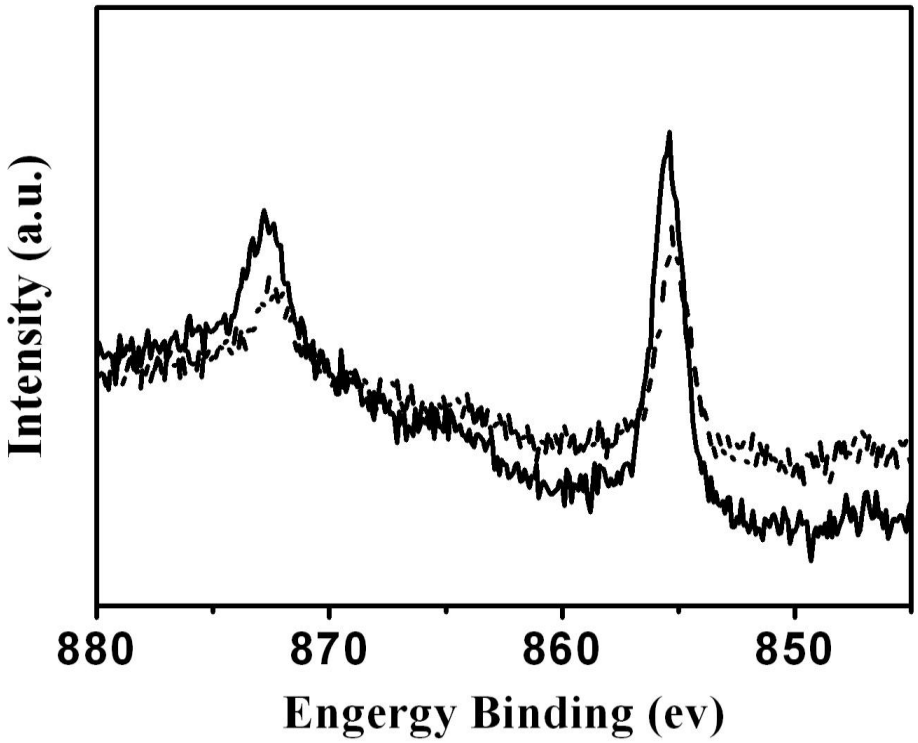

Figure S7. X-ray photoelectron spectra for complex **4** (solid line) and aggregates of complex **4** (dotted dash line) deposited on silicon surface.

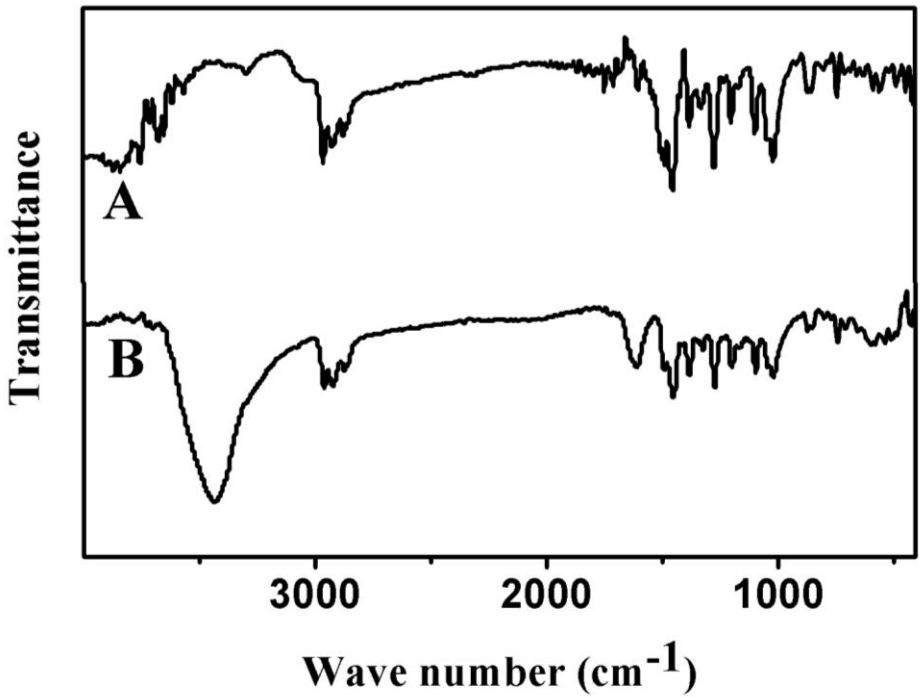

Figure S8. IR spectra of phthalocyanine **1** (A) and nanostructures fabricated from **1** (B) in the region of 400-4000 cm^{-1} with 2 cm^{-1} resolution.

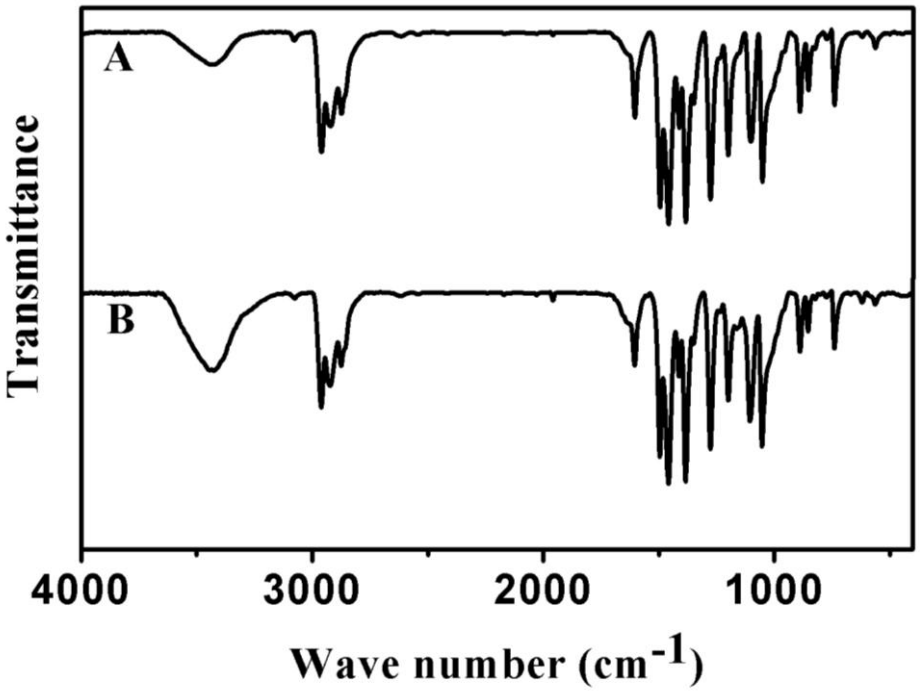

Figure S9. IR spectra of phthalocyanine **2** (A) and nanostructures fabricated from **2** (B) in the region of 400-4000 cm^{-1} with 2 cm^{-1} resolution.

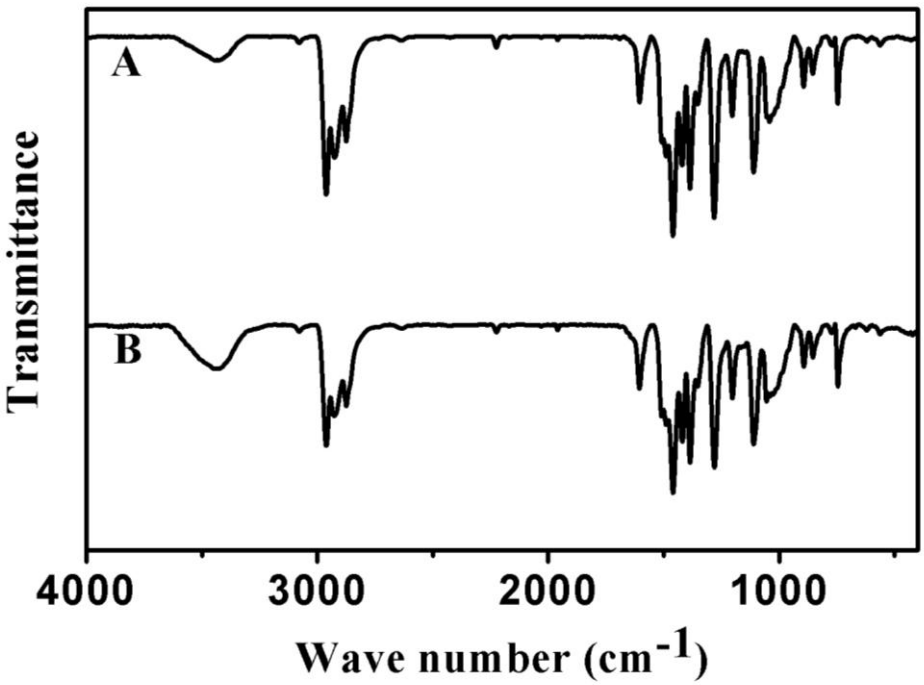

Figure S10. IR spectra of phthalocyanine **3** (A) and nanostructures fabricated from **3** (B) in the region of 400-4000 cm^{-1} with 2 cm^{-1} resolution.

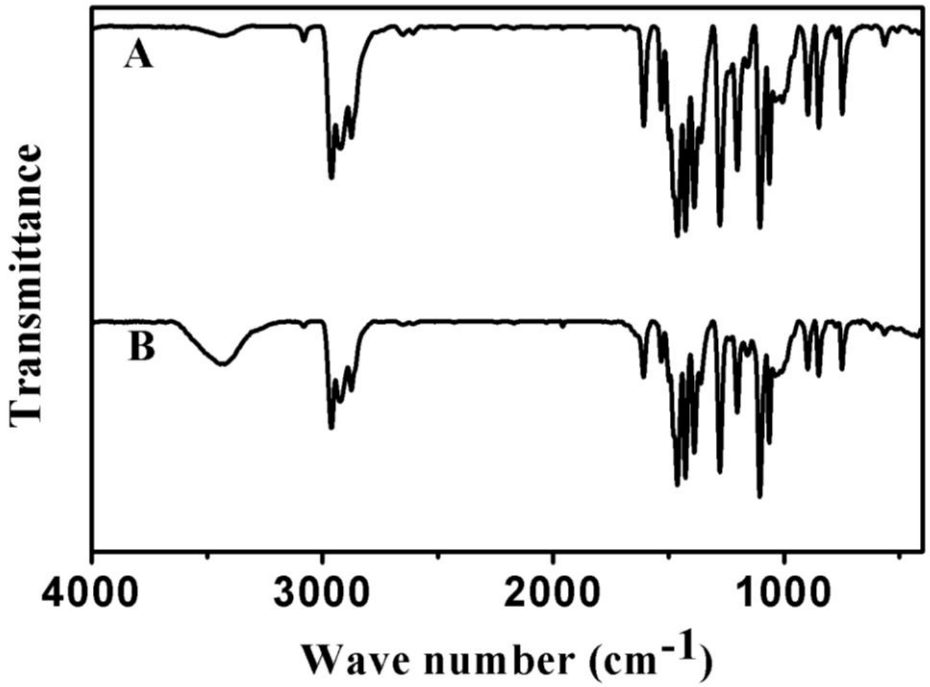

Figure S11. IR spectra of phthalocyanine **4** (A) and nanostructures fabricated from **4** (B) in the region of 400-4000 cm^{-1} with 2 cm^{-1} resolution.

Table S1. Analytical and mass spectroscopic data for the phthalocyanine derivatives 1-4. [a]

Compound	Yield (%)	M^+ (*m/z*)[a,b]	Analysis (%)[a]		
			C	H	N
(*S*) - $H_2Pc(\beta - OC_5H_{11})_8$ (**1**)	33.9	1203.8 (1203.6)	71.90 (71.85)	8.17 (8.21)	9.33 (9.31)
(*S*) - $ZnPc(\beta - OC_5H_{11})_8$ (**2**)	36.6	1266.2 (1266.9)	68.26 (68.25)	7.59 (7.64)	8.89 (8.84)
(*S*) - $CuPc(\beta - OC_5H_{11})_8$ (**3**)	39.2	1265.3 (1265.1)	68.28 (68.35)	7.68 (7.65)	8.81 (8.86)
(*S*) - $NiPc(\beta - OC_5H_{11})_8$ (**4**)	35.5	1259.7 (1260.3)	68.59 (68.62)	7.69 (7.68)	8.83 (8.89)

[a] Calculated values given in parentheses.
[b] By MALDI-TOF mass spectrometry. The value corresponds to the most abundant isotopic peak of the molecular ion (M^+).

Table S2. 1H NMR spectroscopic data (δ) for the compound 1, 2 and 4 recorded in CDCl3. [a]

Compound	Pc-α	Pc-β	Pc NH	Pc alkyl			
				$OCH_2CH(CH_3)C_2H_5$	$OCH_2CH(CH_3)CH_2CH_3$	$OCH_2CH(CH_3)CH_2CH_3$	$OCH_2CH(CH_3)CH_2CH_3$
(*S*) - $H_2Pc(\beta\text{ - }OC_5H_{11})_8$ (**1**)	8.92 (s, 8 H)	4.52-4.39 (t, 16 H)	-0.77 (s, 2 H)	2.23-2.17 (t, 8 H)	1.91-1.80 (t, 16 H)	1.30-1.22 (br, 24 H)	1.17-1.08 (br, 24 H)
(*S*) - $ZnPc(\beta\text{ -}OC_5H_{11})_8$ (**2**)	8.07 (s, 8 H)	4.31-4.25 (t, 16 H)		2.25 (t, 8 H)	1.96 (t, 16 H)	1.37-1.36 (br, 24 H)	1.23-1.21 (br, 24 H)
(*S*) - NiPc $(\beta\text{ -}OC_5H_{11})_8$ (**4**)	8.54 (s, 8 H)	4.44-4.32 (t, 16 H)		2.30-2.19 (t, 8 H)	1.97-1.83 (t, 16 H)	1.49-1.32 (br, 24 H)	1.27-1.15 (br, 24 H)

[a] Multiplicities: s = singlet, d, = doublet, br=broad, m = multiple

Due to the presence of the unpaired electron and the paramagnetic nature of Cu^{2+}, ^1H NMR data for complex **3** is inavailable.

Table S3. Electronic absorption data for the compounds **1-4** in chloroform and their nano-aggregates dispersed in methanol.

Compound	in *chloroform*	in *methanol*
$H_2Pc(\beta\text{-}OC_5H_{11})_8$ (**1**)	294, 346, 424, 588, 622, 646, 681	294, 357, 476, 666
$ZnPc(\beta\text{-}OC_5H_{11})_8$ (**2**)	288, 350, 424, 597, 658	305, 360, 454, 639
$CuPc(\beta\text{-}OC_5H_{11})_8$ (**3**)	297, 337, 401, 603, 662	295, 335, 415, 615, 665
NiPc $(\beta\text{-}OC_5H_{11})_8$ (**4**)	288, 310, 409, 589, 651	272, 328, 428, 605, 673